

# The Effect of Non-Lambertian Surface Reflectance on Aerosol Radiative Forcing

*P. Ricchiazzi, W. O'Hirok, and C. Gautier  
Institute for Computational Earth System Science  
University of California  
Santa Barbara, California*

## Introduction

Surface reflectance is an important factor in determining the strength of aerosol radiative forcing. Previous studies of radiative forcing assumed that the reflected surface radiance is isotropic and does not depend on incident illumination angle. This Lambertian reflection model is not a very good descriptor of reflectance from real land and ocean surfaces. In this study we present computational results for the seasonal average of short and long wave aerosol radiative forcing at the top of the atmosphere and at the surface. The effect of the Lambertian assumption is found through comparison with calculations using a more detailed bi-direction reflectance distribution function (BRDF).

## Method

The SBDART radiative transfer (Ricchiazzi et al 1998) model was used to compute aerosol direct radiative forcing due to aerosols (DRFA; the difference in net radiative flux with and without aerosols) in the shortwave (SW) (0.3-5.0  $\mu\text{m}$ ) and longwave (LW) (5 - 40  $\mu\text{m}$ ) spectral bands. Calculations were performed for four standard aerosol types (d'Almeida et al 1991): 1) Arctic Haze, composed of sulfate, soot and marine aerosol; 2) Continental, composed of soluble, and a small fraction of dust aerosol; 3) Desert Background, composed of mineral particles; and 4) Marine, composed of oceanic and sulfate aerosols. Mie scattering calculations were used to derive optical properties that covered the full spectral range. The impact on the radiative forcing was evaluated for four surface types: 1) fine snow (100  $\mu\text{m}$ ); 2) coarse snow (500  $\mu\text{m}$ ); 3) vegetation; and 4) ocean. The BRDF of the snow models were computed by placing an optically thick layer of ice particles of either 100  $\mu\text{m}$  or 500  $\mu\text{m}$  radius at the bottom of SBDART's computational grid. The vegetation BRDF was modeled using the Ross-thick (Ross 1981) Li-sparse (Li et al 1992) BRDF parameterization measured at SGP (Luo et al. 2003). The measured BRDF parameters were available for only four wavelengths in the SW. A full spectrum model was obtained by extrapolating the BRDF parameters using spectral measurements of grass (Aster spectral library). The ocean BRDF model includes contributions from subsurface water scattering (Morel 1988) and Fresnel reflection from a Gaussian distribution of wave slopes (Cox et al 1956), assuming a wind speed of 5 m/s. The BRDF of the four surface types is shown in Figure 2. In the SW, an additional set of calculations were performed using the directional albedo, instead of the full BRDF treatment. The directional albedo yields the same albedo as the BRDF for the same incident angle, but distributes the reflected radiation isotropically. And finally, a set of calculations were carried out with fully

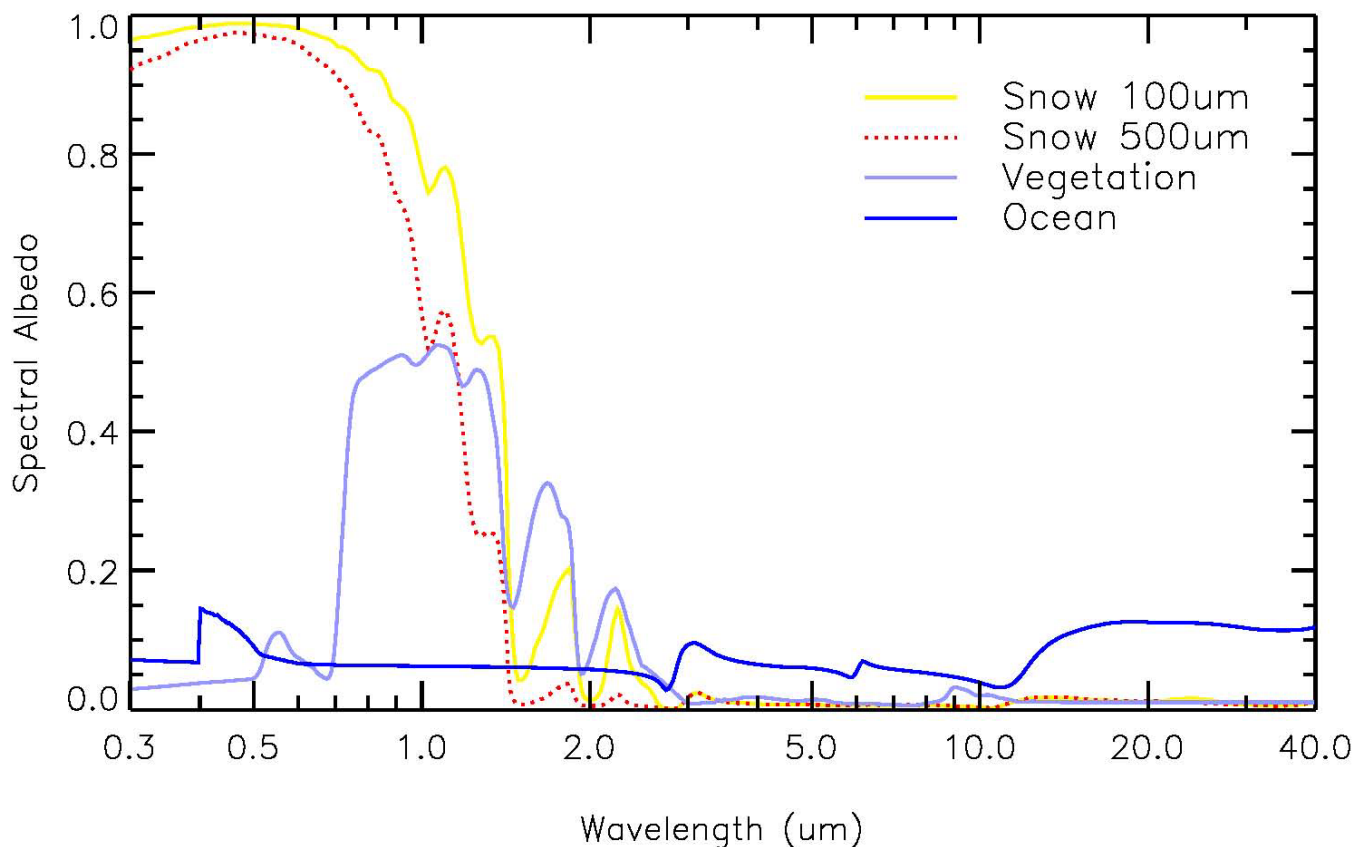


**Figure 1.** Spectral albedo of fine and coarse snow, vegetation and ocean for incident illumination at 60°.

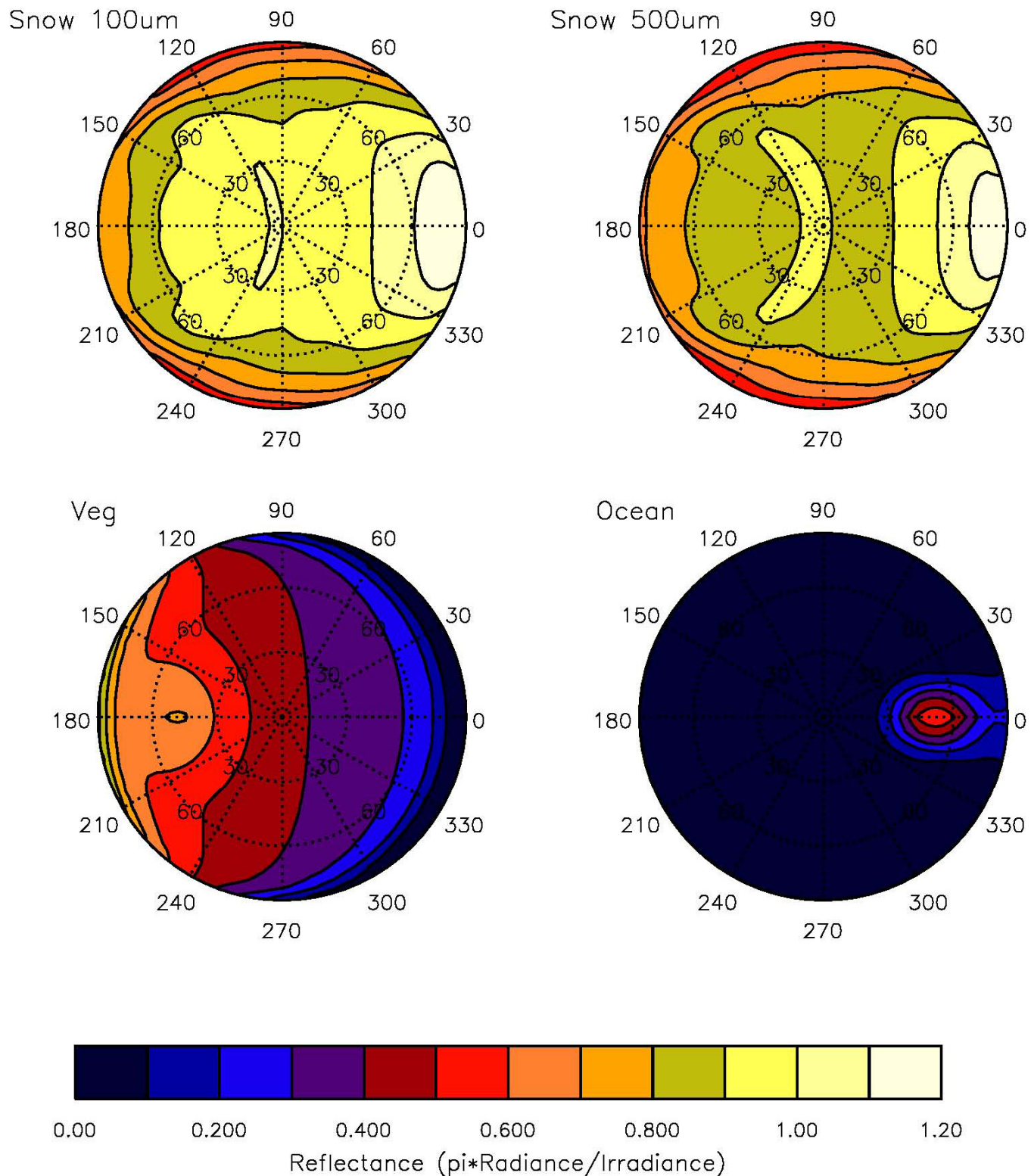


**Figure 2.** BRDF for the four surface types shown if Figure 1, at a wavelength of 750 nm and for an incident illumination angle of 60°.

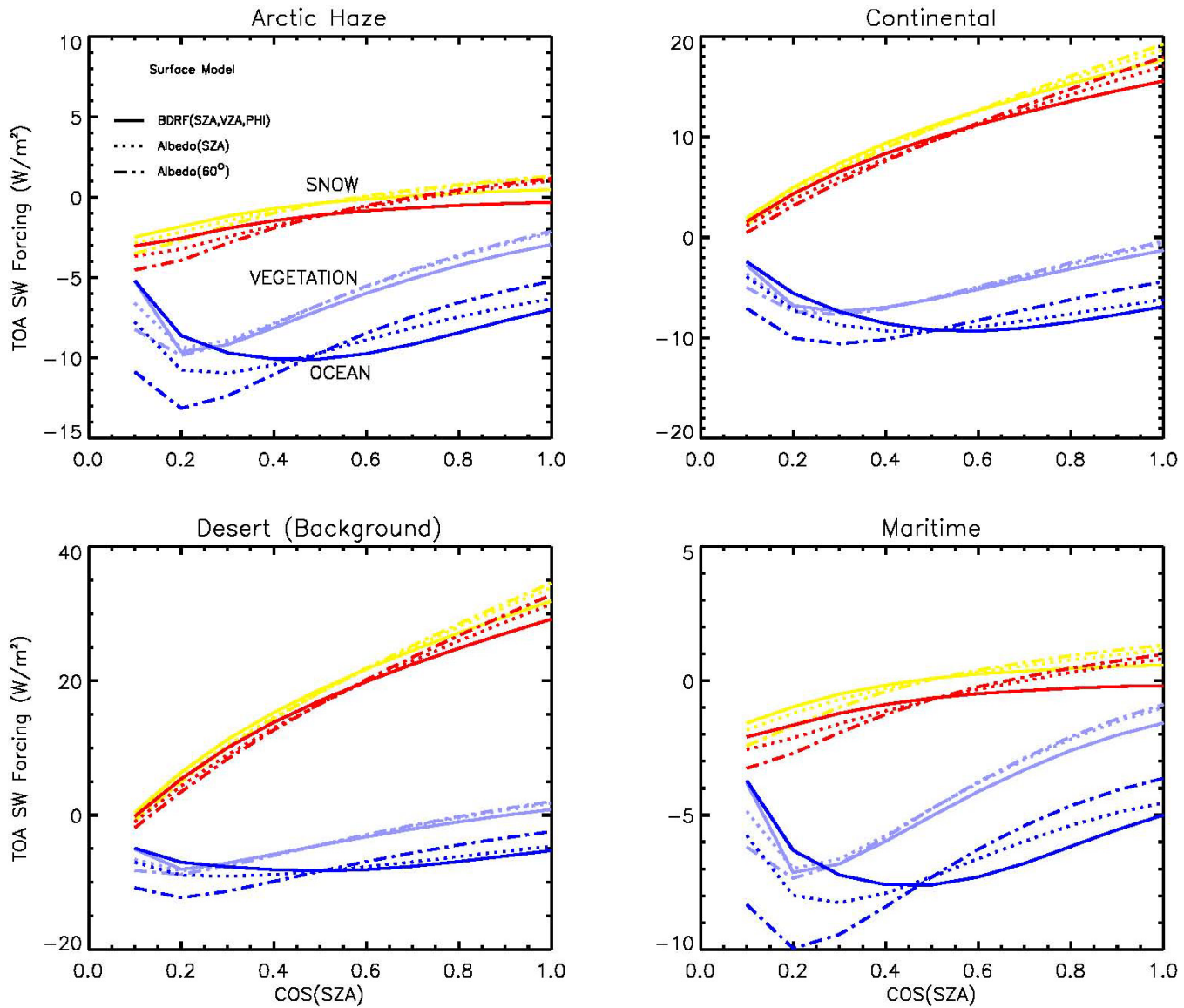


**Figure 3.** Top of the atmosphere (TOA) shortwave aerosol forcing vs solar zenith angle for various aerosol types and surfaces. Three surface models are considered: 1) full BRDF treatment (solid line); 2) directional albedo at the solar zenith angle (dotted line); 3) constant albedo at  $60^\circ$  incident angle (dash-dotted line). Aerosol optical depth is 0.1 at 550 nm.

Lambertian surface reflectance selected to match the albedo of the BRDF for a fixed incidence angle of  $60^\circ$ . After computing the SW radiative forcing at a range of solar zenith (Figure 3), the diurnal average forcing was computed for two time periods: for the 90 day period centered on the Equinox (Figures 4, 6 and 7); and for the 90 day period centered on the N.H. Summer solstice (Figures 5 and 8). All calculations were based on the mid-latitude Summer atmosphere. Therefore, since the LW calculation did not depend on solar zenith angle, the results shown in Figure 9 do not depend on latitude.

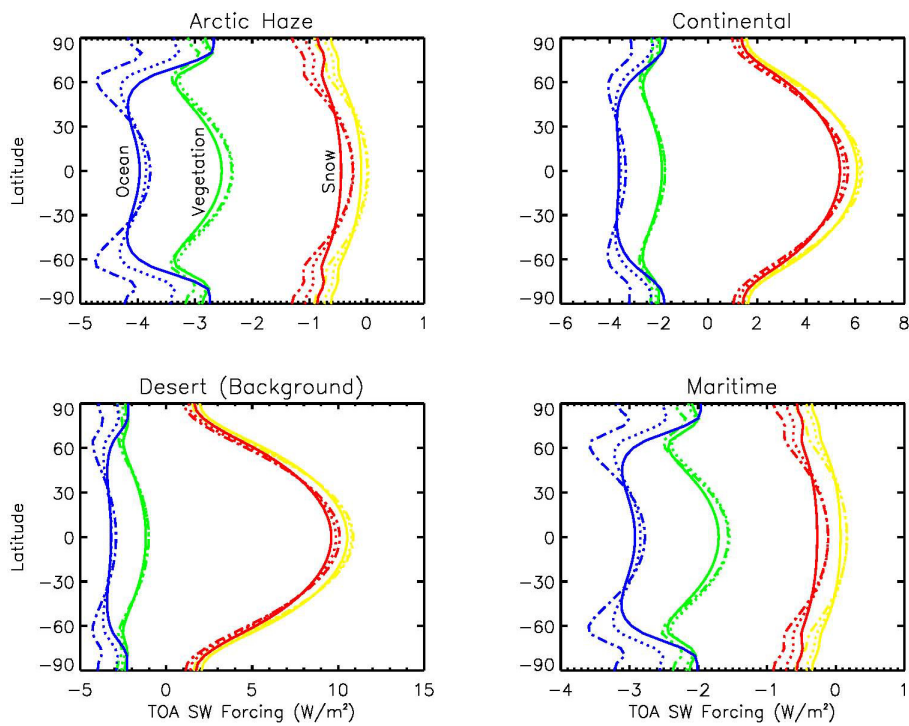


**Figure 4.** TOA shortwave direct radiative forcing due to aerosol vs latitude averaged over a 90 day period centered on the Equinox. The aerosol optical depth is set to 0.1 in all cases, unless otherwise noted.

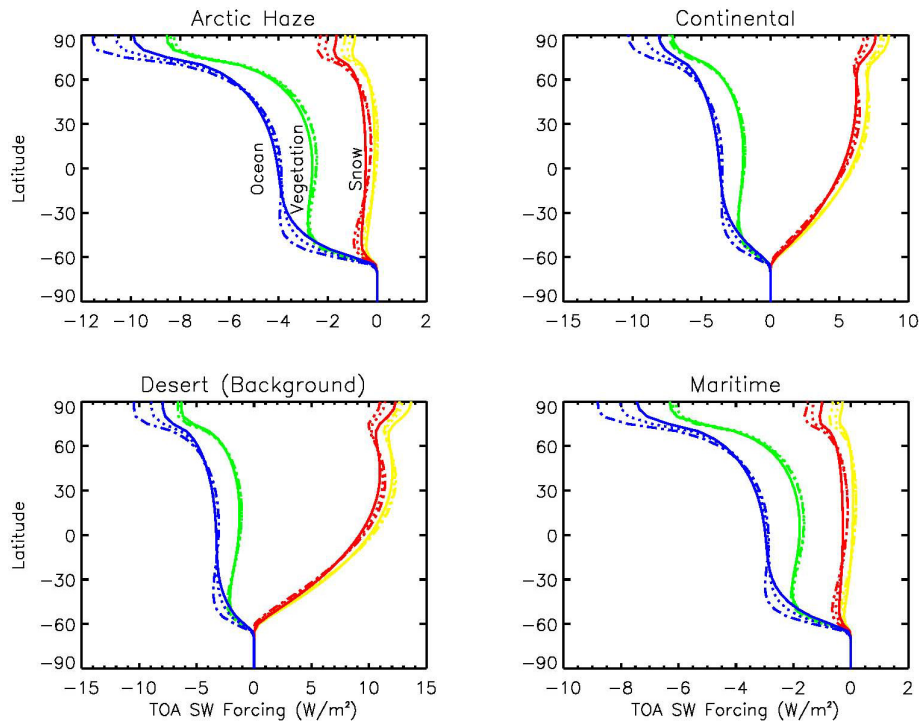


**Figure 5.** TOA SW DRFA for the 90 day period centered on the Summer Solstice.

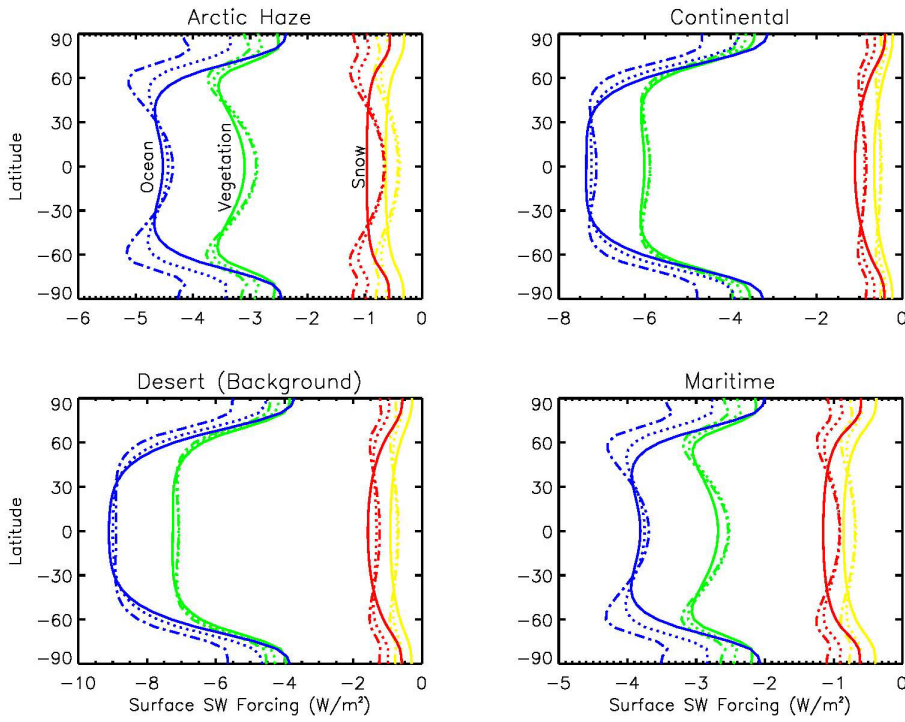


**Figure 6.** A comparison of TOA shortwave forcing over ocean for optical depths of 0.05 and 0.1 for the 90 day period centered on the Equinox.

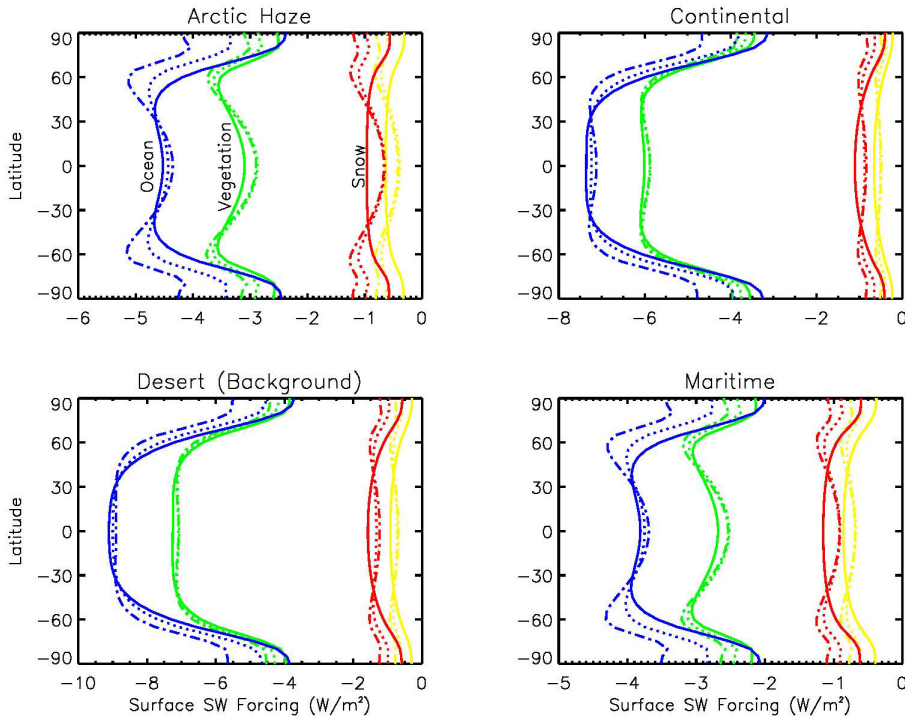


**Figure 7.** Surface SW DRFA averaged over the 90 day period centered on the Equinox.

## Results

As expected, surface type has a large effect on the magnitude and sign of the SW DRFA, with darker surfaces producing more negative forcing. The TOA DRFA is always negative for the Equinox seasonal average, but the Summer Solstice average yields positive forcing with continental or desert aerosol over snow (Figures 4 and 5). The surface DRFA is negative for all aerosol and surface types (Figures 7 and 8). The effect of using the actual BRDF instead of the simpler directional albedo or pure Lambertian models is most noticeable for high latitude regions over ocean. For example, the increased reflectivity of the ocean surface at high angles of incidence (Figure 2) causes the forcing over ocean to match the DRFA over vegetation near the poles (Figures 4 and 7). The difference between the BRDF and the pure Lambertian results is greatest for the Equinox seasonal average because the diurnal average weights the low values of  $\cos(\text{sza})$  more than the Summer Solstice average (e.g., Figures 3, 4, and 5). The importance of this effect is shown if Figure 6, which indicates that the TOA DRFA over ocean using the full BRDF model at an aerosol optical depth of 0.05 is matched in the polar regions by the Lambertian model using an aerosol optical depth of 0.1. Hence, Lambertian models of the ocean surface would tend to overestimate the negative forcing due to aerosol by nearly a factor of two. In most cases the magnitude of the SW forcing is greater than for the LW. (Except, of course, when considering the Southern polar region while using the Summer Solstice seasonal average). Since the surface reflectivity in the LW was close to zero for all the surface types, the emissivity for all surface types was close to one and did not have a strong angular dependence. As shown in Figure 9, the LW DRFA hardly varied when the BRDF model is used instead of the Lambertian approach.

## Conclusions

The assumption of a Lambertian reflectance can lead to biases in modeled aerosol radiative forcing at high latitudes. The magnitude of the offset is significant compared to the overall radiative forcing in polar regions. Polar regions are currently undergoing the most rapid climate change, indicating that they are particularly sensitive to perturbations. It is, therefore, important to improve how models treat the interaction of radiation with the surface at high-incident sun angles.

## References

Aster spectral library: <http://speclib.jpl.nasa.gov/> Reproduced from the ASTER Spectral Library through the courtesy of the Jet Propulsion Laboratory, California Institute of Technology, Pasadena, California. Copyright [encircled "c"] 1999, California Institute of Technology. ALL RIGHTS RESERVED. Source and host: California Institute of Technology, Jet Propulsion Laboratory. Title: ASTER Spectral Library. URL: <http://speclib.jpl.nasa.gov/>. Last updated: unknown. Date accessed: unknown. Editor/author: Dr. Simon J Hook.

Cox C, and WH Munk. 1956. "Slopes of the Sea Surface Deduced from Photographs of Sun Glitter." *Bulletin of the Scripps Institution of Oceanography* 6(9)401-487.

D'Almeida, GA, P Koepke, EP Shettle, eds. 1991. *Atmospheric Aerosols: Global Climatology and Radiative Characteristics*. Hampton, Virginia: A. Deepak Publishing.

- Li, X, and AH Strahler. 1992. "Geometric-Optical Bidirectional Reflectance Modeling of the Discrete Crown Vegetation Canopy: Effect of Crown Shape and Mutual Shadowing." *IEEE Transactions on Geoscience and Remote Sensing* 30(2):276-292.
- Luo, Y., AP Trishchenko, R Latifovic, and Z Li. 2003. "Surface Bi-Directional Reflectance Properties Over the ARM SGP Area from Satellite Multi-platform Observations." In *Preceding of the Thirteenth ARM Science Team Meeting*, Broomfield, Colorado, March 31-April 4.
- Morel, A, 1988. "Optical Modeling of the Upper Ocean in Relation to its Biogenous Matter Content (Case-I Waters)." *Journal of Geophysical Research- Oceans* 93(C9)10749-10768.
- Ricchiazzi, P, S Yang, C Gautier, D Sowle. 1998. "SBDART: A Research and Teaching Software Tool for Plane-Parallel Radiative Transfer in the Earth's Atmosphere." *Bulletin of the American Meteorological Society*. 79(10):2101–2114.
- Ross, JK. 1981. *The Radiation Regime and Architecture of Plant Stands, Tasks for Vegetation Sciences* v3. The Hague, London: W. Junk Publishers. 392pp.